953-12-8; **2d**, 949-88-2; **2e**, 7466-30-0; **2f**, 137720-86-6; **2g**, 137720-87-7; **2h**, 6311-55-3; **2i**, 137720-88-8; **2j**, 7400-25-1; **2k**, 137720-89-9; **2l**, 17999-52-9; **2m**, 137720-90-2; **2n**, 137720-91-3; **2o**, 137720-92-4; **2p**, 137721-01-8; **2q**, 20217-91-8; **2r**, 137721-02-9; **2s**, 137721-03-0; **3**, 1019-13-2; **4**, 17049-65-9; **5**, 18428-89-2; **6**, 3682-71-1; **7a**, 54184-69-9; **7b**, 137720-93-5; **7c**, 137720-94-6; **8**, 16288-73-6; **9**, 93-63-0; **10**, 2866-82-2; **11**, 137721-00-7; **12**, 71903-22-5; **13**, 137721-04-1; **14a**, 137721-05-2; **14b**, 137721-06-3; **14c**, 137721-07-4; **15a**, 137721-08-5; **15b**, 137721-09-6; **16a**, 137721-10-9; **16b**, 137721-11-0; **16c**, 137721-12-1; Bu_3SnH, 688-73-3; Ph_3SiH, 789-25-3; Ph_3GeH, 2816-43-5; Bu_6Sn_2, 813-19-4; 4-(phenylazo)phenol, 1689-82-3; 3-(phenylazo)phenol, 2437-11-8; 2-amino-2′-iodobiphenyl, 54147-90-9; 4-(nitrosomethyl)benzene, 623-11-0; 3,5-dimethoxybenzenamine, 10272-07-8; 1-(2-aminophenyl)ethanone, 25384-14-9; 1-hydroxynaphthalene, 90-15-3; 1-[2-[(4-hydroxy-1-naphthalenyl)azo]phenyl]ethanone, 137720-98-0; (4-hydroxyphenyl)phenyldiazene, 51451-39-9; (3-hydroxyphenyl)phenyldiazene sodium salt, 137720-99-1; chlorotriphenylmethane, 76-83-5; triphenylmethane, 519-73-3; 1-[(3-triphenylmethoxy)phenyl]-2-phenylhydrazine, 137721-13-2.

Mechanism of Oxygen Atom Transfer from Oxaziridine to a Lithium Enolate. A Theoretical Study

Robert D. Bach* and José L. Andrés

Department of Chemistry, Wayne State University, Detroit, Michigan 48202

Franklin A. Davis

Department of Chemistry, Drexel University, Philadelphia, Pennsylvania 19104

Received January 9, 1991

The asymmetric enolate oxidation protocol employing enantiopure *N*-sulfonyloxaziridines is highly successful in the synthesis of enantiomerically enriched α-hydroxy carbonyl compounds. Molecular orbital calculations at the HF/6-31+G*//HF/4-31+G level have been used on a model system to elucidate the structural and electronic features of the transition state for oxygen atom transfer. Oxidation of the lithium enolate of acetaldehyde proceeds by S_N2 attack of the β-carbon on the enolate along the O–N bond of the parent oxaziridine. In the transition state the lithium cation is coordinated to both the enolate and the oxaziridine oxygen atoms. Model studies suggest that the sulfonyl oxygen atom is also bound to the metal cation, influencing the stereoselectivity of the resulting α-hydroxy carbonyl compound.

Introduction

The asymmetric synthesis of α-hydroxy carbonyl compounds is a subject of considerable current interest because this structural unit is featured in many natural products.[1] Furthermore these compounds are useful chiral building blocks in the synthesis of biologically active materials.[2] An important strategy in the chiral synthesis of these materials is the asymmetric α-hydroxylation of an enolate anion using an enantiomerically pure (camphorylsulfonyl)oxaziridine, **1**, oxidizing reagent (eq 1).[1,3,4] Stereoselectivities

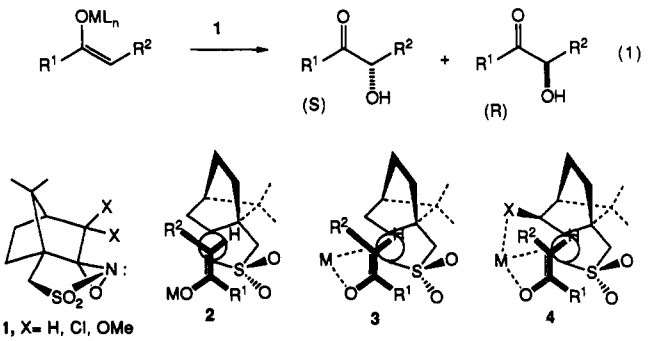

for oxygen transfer of better than 95% ee are often realized.[1,4–6] From the structure reactivity trends the results were generally interpreted in terms of an "open" transition state dominated by nonbonded steric interactions with minimal direct influence of the metal cation, i.e. **2**.[1,3,5] In this model the reasonable assumption was made that the metal oxygen moiety is the sterically most demanding group in the region of the enolate anion.

While this simple model has proven useful in rationalizing the molecular recognition, in many cases the stereoselectivities are frequently unpredictable. Recent studies have shown that the absolute stereochemistry of the products are dependent upon (i) the structure of the enolate, (ii) the oxidant, and (iii) the reaction conditions.[1,3] Undoubtedly this imprecision is related to a lack of knowledge of the transition-state structures (TS) as well as difficulty in relating the aggregated solution structure of the enolate to its reactivity.[3] Recent studies of the asymmetric oxidation of tetralone enolate derivatives using **1** (X = Cl or OMe) has suggested the possibility of transition-state stabilization via chelation of the metal enolate with the oxaziridine **3** or a substituent X, **4**; i.e. a "closed" transition state.[1,4,6]

In earlier theoretical studies on oxygen atom transfer from oxaziridine to an alkene,[7a] one of the major objectives was to identify any electronic effects pertaining to the approach of the reactants that would favor a planar versus a spiro transition state (Figure 1). It had been anticipated[7a] that the higher energy π-type lone pair on the oxaziridine oxygen could interact with the π* orbital of the alkene undergoing epoxidation in a spiro orientation resulting in a two-electron stabilization of the TS. At the

(1) Davis, F. A.; Sheppard, A. C.; Chen, B. C.; Haque, M. S. *J. Am. Chem. Soc.* **1990**, *112*, 6679.
(2) Hannessian, S. *Total Synthesis of Natural Products: the Chiron Approach*, Pergamon Press; New York, 1983; Chapter 2.
(3) For a review on the chemistry of *N*-sulfonyloxaziridines which includes a section on enolate oxidations by these reagents, see: Davis, F. A.; Sheppard, A. C. *Tetrahedron* **1989**, *45*, 5703.
(4) (a) Davis, F. A.; Weismiller, M. E. *J. Org. Chem.* **1990**, *55*, 3715. (b) Davis, F. A.; Chen, B.-C. *Tetrahedron Lett.* **1990**, *31*, 6823.
(5) Chen, B.-C.; Weismiller, M. C.; Davis, F. A.; Boschelli, D.; Empfield, J. R.; Smith, A. B. III *Tetrahedron* **1991**, *47*, 173.
(6) Davis, F. A.; Kumar, A.; Chen, B.-C. *J. Org. Chem.* **1991**, *56*, 1143.
(7) (a) Bach, R. D.; Wolber, G. J. *J. Am. Chem. Soc.* **1984**, *106*, 1410. (b) Bach, R. D.; Coddens, B. A.; McDouall, J. J. W.; Schlegel, H. B.; Davis, F. A. *J. Org. Chem.* **1990**, *55*, 3325.

0022-3263/92/1957-0613$03.00/0

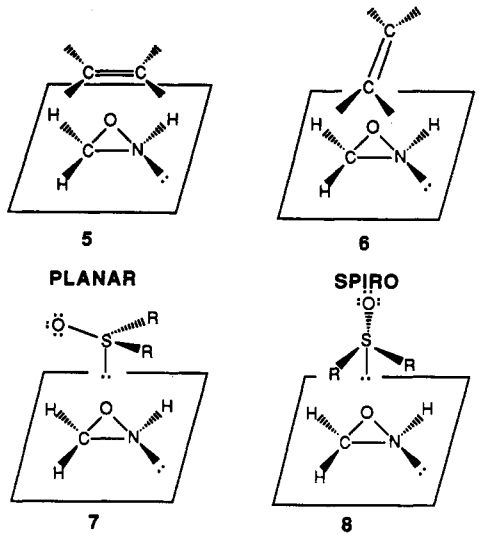

Figure 1. Transition states for oxygen transfer from an oxaziridine to an alkene and a sulfoxide.

HF/6-31G* level of theory we found identical activation barriers (57.6 kcal/mol) for both first-order saddle points **5** and **6**.[7b]

The barriers for the planar **7** (31.1 kcal/mol) and spiro **8** (31.5 kcal/mol) transition structures for oxidation of the parent sulfoxide (H_2SO) differed by only 0.4 kcal/mol (MP4SDTQ/4-31G(d)). From these data it was concluded that the enantioselectivity observed with chiral oxidants[3] should be attributed largely to steric effects arising from substituents on both the oxaziridine and on the substrates. In both cases the geometry of the nucleophilic substrate being oxidized had undergone only minor changes at the TS while that of the oxaziridine had been extensively perturbed with its O–N and O–C bonds being elongated by 30 and 40% relative to their ground-state geometries. The apparent electronic indifference of these model transition structures to orientation of approach of the reactants may be attributed to the relatively long bond distances between the "electrophilic" oxygen and its reacting partners. A qualitative feature that each of these transition structures has in common is that they resemble a singlet oxygen atom suspended between the developing CH_2=NH departing fragment and the attacking nucleophile. Since two of the lone pairs of electrons on the central oxygen would be nearly degenerate in such a geometric array, one should not anticipate a stereoelectronic preference for a spiro transition state.

We have made a similar observation for oxygen atom transfer from hydrogen peroxide[8] (Figure 2). The gas phase oxidation of ammonia by H_2O_2 is a two-step process first involving a 1,2-hydrogen shift with a subsequent oxygen atom transfer from water oxide (H_2O^+–O^-). The high barriers for **9** and **10** are a consequence of the energetic requirements of the 1,2-hydrogen shift in H_2O_2 (56.0 kcal/mol) prior to the oxygen transfer step.[8] This rearrangement is essential to the overall oxidation mechanism because of the requirements of a neutral leaving group (H_2O). Epoxidation of an alkene by a peroxy acid, however, occurs by an entirely different pathway. In TS-**11** the hydrogen on peroxyformic acid is fully bonded to the electrophilic oxygen ($r(O_1H_1)$ = 1.00 Å) in the transition

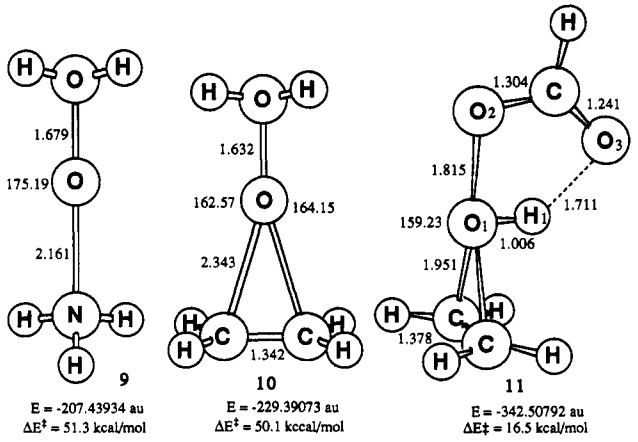

Figure 2. Transition structures (MP4SDTQ/6-31G*//MP2/6-31G*) for oxygen transfer from hydrogen peroxide (water oxide) to ammonia and ethylene and for epoxidation of ethylene by peroxyformic acid.

Table I. Total Energies (au) for Reactants, Products, and the Transition State for Oxygen Atom Transfer

	level of theory		
	HF/3-21G	HF/4-31+G	HF/6-31+G*//HF/4-31+G
oxaziridine **12**	-167.85168	-168.54336	-168.808682
methyleneamine **13**	-93.49478	-93.88904	-94.031907
lithium enolate **14**	-158.91162	-159.60193	-159.806448
lithium alkoxide **15**	-233.38460	-234.36859	-234.694381
reactants complex **16**	-326.82457	-328.18341	-328.647580
products complex **17**	-326.92787	-328.29786	-328.759291
TS-1	-326.77283	-328.13270	-328.579369

state and the hydrogen is transferred to the carbonyl oxygen affording neutral formic acid *after the barrier is crossed*. Electronic differentiation between the two orthogonal oxygen lone pairs (σ and π) which typically differ in energy by as much as 31 kcal/mol results in a 9.2 kcal/mol preference for a symmetrical spiro transition state[8c] (MP4SDTQ/6-31G*//MP2/6-31G*). However, we have recently found a TS that is even lower in energy (0.23 kcal/mol) where the peroxy acid approaches the double bond of ethylene in an unsymmetrical manner directly over one of the methylene carbon atoms.[8e]

In the present theoretical study we seek the underlying reasons for the remarkably high enantioselectivity observed in the asymmetric oxidation of enolate anions with chiral oxaziridines. We specifically wish to address the question about the role of the lithium cation and whether the oxygen would approach the enolate anion in an unsymmetrical fashion by bonding principally to one carbon atom or whether the TS more closely resembles an epoxide.

Results and Discussion

Molecular-orbital calculations have been carried out initially at the HF/3-21G level of approximation using the GAUSSIAN-88 program system[9] utilizing gradient geometry optimization.[9c] Preliminary geometries were then refined by full geometry optimization at HF/4-31+G[9d] and sin-

(8) (a) Bach, R. D.; McDouall, J. J. W.; Owensby, A. L.; Schlegel, H. B. *J. Am. Chem. Soc.* **1990**, *112*, 7065; (b) **1990**, *112*, 7064. (c) Bach, R. D.; Owensby, A. L.; González, C.; Schlegel, H. B.; McDouall, J. J. W. *J. Am. Chem. Soc.* **1991**, *113*, 2338; (d) **1991**, *113*, 6001. (e) Unpublished results.

(9) (a) Molecular orbital calculations have been carried out using the GAUSSIAN 88 program system[9b] utilizing gradient geometry optimization.[9c] (b) Frisch, M. J.; Head-Gordon, M.; Schlegel, H. B.; Raghavachari, K.; Binkley, J. S.; González, C.; DeFrees, D. J.; Fox, D. J.; Whiteside, R. A.; Seeger, R.; Melius, C. F.; Baker, J.; Martin, R. L.; Kahn, R. L.; Stewart, J. J. P.; Fluder, E. M.; Topiol, S.; Pople, J. A. *Gaussian 88*; Gaussian, Inc.: Pittsburgh, PA, 1988. (c) Schlegel, H. B. *J. Comp. Chem.* **1982**, *3*, 214. (d) Chandrasekhar, J.; Andrade, J. G.; Schleyer, P. v. R. *J. Am. Chem. Soc.* **1981**, *103*, 5609. (e) Clark, T.; Chandrasekhar, J.; Spitznagel, G. W.; Schleyer, P. v. R. *J. Compt. Chem.* **1993**, *4*, 294. (f) González, C.; Schlegel, H. B. *J. Chem. Phys.* **1989**, *90*, 2154.

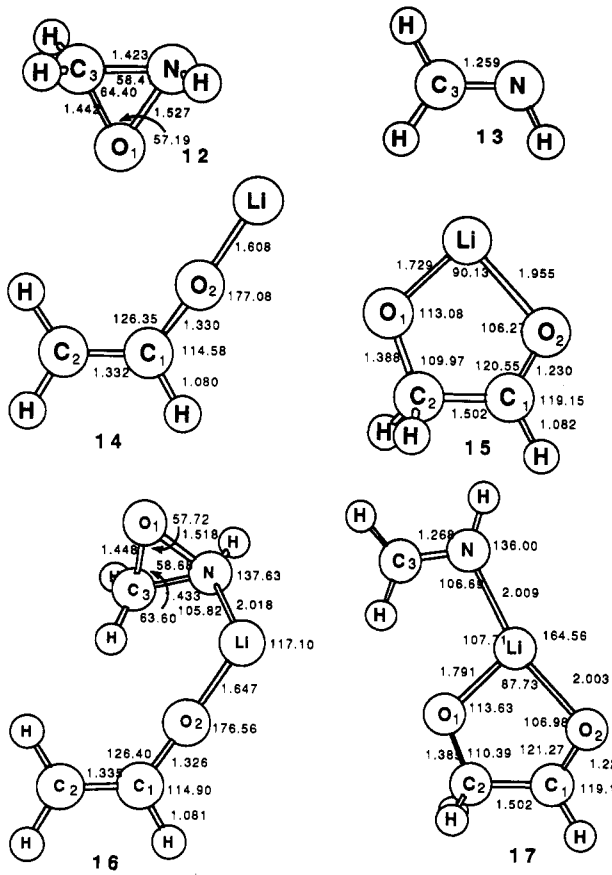

Figure 3. Geometries for reactants and products of oxygen atom transfer from lithium enolate anion of acetaldehyde (HF/4-31+G).

gle-point calculations at the HF/6-31+G*[9e] level were carried out on the HF/4-31+G geometries to insure better energies for this anionic transition state (Table I). The structure of lithium enolate **14** posed a unique problem in that the minimum structure with the 3-21G basis has the lithium out of the plane defined by atoms C_2–C_1–O_1 and that it bonds to the oxygen and C_1 in a π-allylic sense, while the 4-31+G basis set gives a nearly linear C–O–Li in the plane as shown in Figure 3. The situation is further complicated by the prior report that the former structure is favored by 1.44 kcal/mol when d orbitals are included in the basis set.[10] Since the energy differences are relatively small and do not directly affect the mechanistic considerations in question, we will utilize **14** as the structure of the starting material or reactant. The total energies at all three levels of theory are given in Table I, and the structures for the reactants and products are given in Figure 3. As noted in Figure 4 the calculated energy differences between reactants and products, as well as the activation barriers, are surprisingly close when the three levels of theory are compared despite the inclusion of diffuse sp functions and the polarization functions in the basis sets. The most significant change at the HF/6-31+G* level is the increase in the activation barrier ($\Delta E^{\ddagger}$ = 22.4 kcal/mol) for TS-1. Although the transition structure is only 22.4 kcal/mol above isolated reactants, TS-1 is 42.8 kcal/mol higher in energy than reactant complex **16**. The magnitude of the calculated barrier is sufficiently high that solvation effects must play a major role in order to affect oxidation at the low temperatures (~−40 °C) typically employed in the laboratory. The overall reaction is highly exothermic (~70 kcal/mol), reflecting the release of strain energy in the oxaziridine and the formation of both C=N and C=O π-bonds. Both reactant and product complexes exhibit a surprisingly high degree of stabilization (~20 kcal/mol). However, in the absence of the plus basis set this stabilization appears to be greatly exaggerated. The two levels of theory also give remarkably similar transition-state geometries. Vibrational frequencies were calculated by using analytical second derivatives for the transition structure (TS-1) at both levels of theory. The observation of one imaginary frequency establishes first-order saddle point TS-1 to be a real transition state. As one might anticipate, the lithium cation is bridged between the two oxygens in the product lithium alkoxide **15**, and the lithium is more strongly bonded to nitrogen than to oxygen in clusters **16** and **17** based upon a Mulliken population analysis.

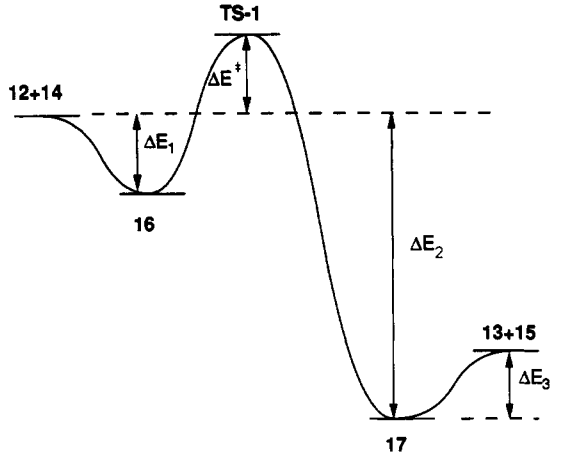

Energy Differences	HF/3-21G	HF/4-31+G	HF/6-31+G*//HF/4-31+G
ΔE_1	-38.4	-23.9	-20.4
$\Delta E^{\ddagger}$	-6.0	7.0	22.4
ΔE_2	-103.3	-95.7	-90.5
ΔE_3	30.4	25.2	20.7

Figure 4. Potential energy surface for oxygen atom transfer from oxaziridine to the lithium enolate anion of acetaldehyde, relative energies are in kilocalories/mole.

Significant structural reorganization is required of reactant cluster **16** enroute to the transition state. In TS-1 the β-carbon C_2 of enolate **14** must become nearly aligned with the backside of the O_1–N bond axis to effect a displacement of CH_2=NH in an S_N2 fashion. This is consistent with frontier MO concepts since the largest coefficient in the HOMO of **14** is at C_2. The orbital splitting attending the resonance interactions of the lone pair of electrons on oxygen with the π-bond results in a HOMO orbital (−0.277 au) in **14** that is 2.94 eV (67.8 kcal/mol) higher in energy that the corresponding π orbital (−0.168 au) in ethylene (HF/4-31+G). As discussed previously[7] the LUMO of the oxaziridine is a Walsh-type orbital that is highly electrophilic due to a facile O–N and O–C bond elongation when a nucleophile attacks the "electrophilic" oxygen. The electrophilic properties of the oxaziridine ring, that bears three pairs of unpaired electrons, may be attributed to the σ^* components of this virtual Walsh orbital that can rapidly decrease in energy early along the reaction coordinate as a result of the relatively weak O–N bond. The HOMO–LUMO energy gap (9.6 eV) is relatively small due to the increase in HOMO of lithium enolate **14**. This also means that this nucleophilic HOMO

(10) Lynch, T. J.; Newcomb, M.; Berbreiter, D. E.; Hall, M. B. *J. Org. Chem.* **1980**, *45*, 5005.

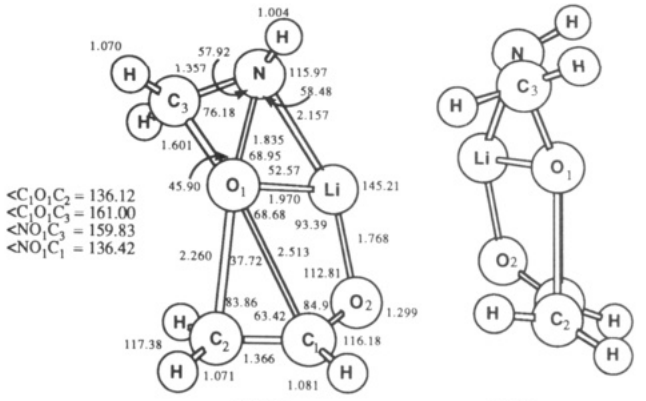

Figure 5. (a, left) Geometry for the transition structure for oxygen transfer from oxaziridine to the lithium enolate of acetaldehyde (HF/4-31+G). (b, right) An end-on view of the transition structure rotated 90°. The dihedral angle defined by the central oxygen and the C–N bond and the C–C bond is ~160°.

is considerably higher in energy (146.8 kcal/mol) than the HOMO of oxaziridine which reduces the closed-shell repulsion, and the HOMO–HOMO orbital splitting in TS-1 is surprisingly small (~14.4 kcal/mol). Consequently the net three-MO four-electron stabilization is less than 1 kcal/mol.[7] The enthalpy of activation is reduced by the attendant carbon–nitrogen π-bond formation.

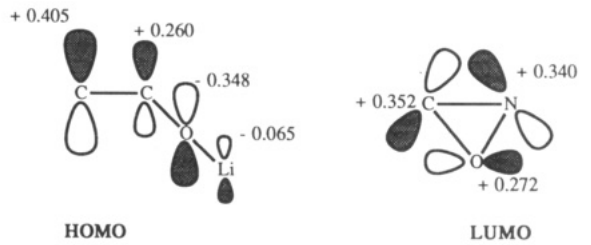

The most revealing feature of TS-1 is the significant role played by the lithium cation in ensuring the alignment of the interacting fragments (Figure 5). Early along the reaction coordinate the negative charge resides largely on the enolate oxygen (O_2). Since the negative charge must be transferred to the alkoxide oxygen (O_1) in the product, the primary allegiance of bonding of the lithium cation must be transferred from O_2 to O_1 along the reaction pathway in order to avoid the intermediacy of an energetically unfavorable "naked" oxyanion. Although the nitrogen remains bonded to the lithium cation throughout the reaction and serves to hold the C–N and C–C bonds in a nearly coplanar arrangement, it is more strongly bound to nitrogen in **16** and **17** than in TS-1 based upon the Mulliken population analysis. The dihedral angle between the two interacting planes of ~160° (Figure 5b) is probably a reflection of geometric distortion in order to maximize the simultaneous bonding of the lithium cation to both oxygens. The bonding of the transferrable oxygen (O_1) to the β-carbon (C_2) of the enolate is relatively weak and is estimated to be ~5% based upon a Mulliken population analysis. The interaction of the electrophilic oxygen O_1 with the α-carbon (C_1) is slightly antibonding. The calculated charge on O_1 in oxaziridine is −0.339 while that electron density has been reduced to −0.133 in TS-1. In contrast to oxidation of a sulfoxide where 0.54 electrons were transferred from H_2SO to the oxaziridine moiety in **7**, only 0.12 electrons were transferred from the lithium enolate to the oxaziridine in TS-1.

In order to get a more realistic view of the actual bonding interactions of an enolate anion with a chiral sulfonamide

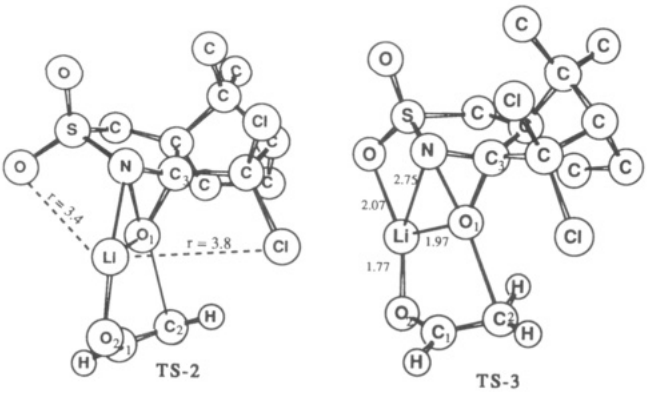

Figure 6. Two orientations of approach of lithium enolate **14** to (camphorylsulfonyl)oxaziridine **1** (X = Cl) in the transition state for oxygen atom transfer.

(**1**, X = Cl), we took the geometry of **1** from an X-ray analysis[11] and embellished it by replacing the two hydrogens at C_8 with two chlorine atoms (using standard bond angles and distances). We then appended enolate anion **14** using the ab initio geometry of TS-1. Consideration of the two enantiofaces of the lithium enolate places the enolate oxygen (O_2) away from the endo face of the camphoryl moiety in TS-**2** and pointed toward the SO_2 group in TS-**3**. Geometry optimization of the resulting "transition structures" (Figure 6) is obviously prohibitive due to their size, although for a system this rigid, the crude assembling of the two fragments appears to be a reasonable approximation. The lithium–chlorine and lithium–sulfonyl oxygen bond distances in TS-**2** are 3.8 and 3.4 Å, respectively, in this idealized geometry. The optimized lithium chloride bond distance in a $H_3CCl\cdots Li^+$ complex is 2.35 Å with a C–Cl–Li^+ bond angle of 120.8° and a stabilization energy of 21.6 kcal/mol (HF/6-31G*).[12] Although these distances in TS-**2** are too long to represent effective bonds, it appears that solvent would be sterically precluded from this chiral cavity on the endo face of the bicyclic ring. There does appear to be room for solvation of the lithium cation on the front face of TS-**2**. The steric requirements of TS-**2** further suggest that a monomeric lithium enolate is involved in the TS and that the face selectivity of oxidation is determined largely by steric factors.

A slight twisting about the O_1–C_2 bond in TS-**2** would bring the lithium cation sufficiently close to the sulfonyl oxygen to result in significant TS stabilization. Despite the fact that sulfonyl oxygens are only weak Lewis base sites,[14] metal chelation involving them has often been invoked as an element of transition-state control[15] and in one example for enolate oxidations by chiral *N*-sulfonyloxaziridine.[16] Furthermore, Oppolzer has presented evidence that chelation involving a sulfonyl oxygen and a carbonyl group are responsible for the high diastereoselectivities observed in the Lewis acid catalyzed inter- and

(11) Davis, F. A.; Towson, J. C.; Weismiller, M. C.; Sankar, L.; Carroll, P. J. *J. Am. Chem. Soc.* **1988**, *110*, 8477.

(12) The stabilization of CH_3F complexed to lithium cation is 35.1 kcal/mol. In this case the C–F–Li^+ bond angle is 180.0° and the Li–F bond distance is 1.74 Å. Experimental lithium affinities for CH_3Cl and CH_3F are 24 and 31 kcal/mol, respectively.[13]

(13) Staley, R. H.; Beauchamp, J. L. *J. Am. Chem. Soc.* **1975**, *97*, 5920.

(14) Davis, F. A.; Towson, J. C.; Weismiller, M. C.; Sankar, L.: Carroll, P. J. *J. Am. Chem. Soc.* **1988**, *110*, 8477.

(15) For examples of metal chelation involving sulfonyl oxygens, see: Trost, B. M.; Schmuff, N. R. *J. Am. Chem. Soc.* **1985**, *107*, 396. Hellwinkel, D.; Lenz, R.; Lammerzahl, F. *Tetrahedron* **1983**, *39*, 2073. Giblin, G. M. P.; Simpkins, N. S. *J. Chem. Soc., Chem. Commun.* **1987**, 207. Hollstein, W.; Harms, K.; Marsch, M.; Boche, G. *Angew. Chem., Int. Ed. Engl.* **1987**, *26*, 1287.

(16) Davis, F. A.; ThimmaReddy, R.; McCauley, J. P., Jr.; Przeslawski, R. M.; Harakal, M. E.; Carroll, P. J. *J. Org. Chem.* **1991**, *56*, 809.

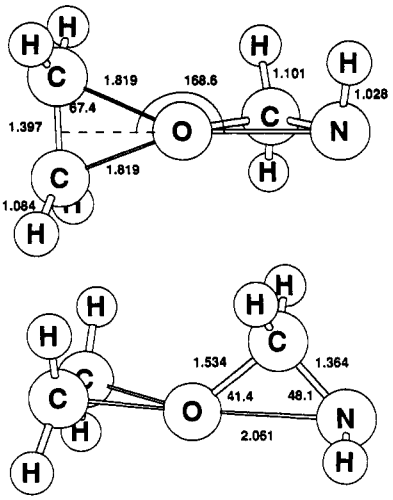

Figure 7. Two different orientations of the transition structure (TS-4) for oxygen atom transfer from oxaziridine to ethylene at MP2/6-31G*.

intramolecular Diels–Alder reactions of *N*-enoylbornane-10,2-sultams.[17]

In TS-3 the lithium cation is much closer (2.07 Å) to the sulfonyl oxygen and should provide a greater degree of stabilization. In TS-3 if the hydrogen atom syn to the enolate oxygen (O_2) is placed under the bicyclic carbon skeleton as steric considerations clearly indicate, then an *E*-enolate may be more easily accomodated in the TS than a *Z*-enolate. However, the available evidence, based upon enolate trapping experiments, suggest that the *Z*-enolate is involved. It is also quite conceivable that the oxygen could be transferred to the opposite stereoface of the enolate in TS-2, which would place the O_2–Li moiety closer to the chlorine. This interesting question must await additional investigation.

Since the basic precept of a spiro TS requires a nearly symmetrical bonding interaction of a π-type oxygen lone pair with the π^* orbital of the carbon–carbon double bond, the unsymmetrical approach of the oxygen atom in TS-1 negates any consideration of a preferential interaction of one of the oxygen lone pairs with the π^* orbital of the enolate anion. The essential features of both transition structures (Figure 6) are that the β-carbon (C_2) must align itself along the O–N bond to effect an S_N2 displacement at oxygen and that rotation about the developing C_2–O_1 bond can occur to minimize steric interactions with the proviso that the lithium cation can maintain effective bonding to *both* oxygen atoms throughout the reaction pathway.

Since the unsymmetrical nature of the approach of the oxygen to the carbon–carbon double bond in TS-1 is in contrast to that observed in **5** and **6**, we elected to examine this model oxidation at a higher level of theory. Previous experience[8] with hydrogen peroxide and peroxyformic acid suggested that geometry optimization at the MP2/6-31G* level gave a much "tighter" transition structure. The transition state for formation of ethylene oxide (TS-4) at the MP4SDTQ/6-31G*//MP2/6-31G* level had a barrier of 37.0 kcal/mol. The approach to the double bond was indeed symmetric, but the S_N2 displacement by the π-bond took place along the O–N bond axis (Figure 7). Thus, TS-4 has the O–N bond breaking further advanced than O–C bond elongation as noted above in TS-1. The change in transition-state structure relative to **6** is a reflection of

(17) Oppolzer, W.; Rodriguez, I.; Blagg, J.; Bernardinelli, G. *Helv. Chim. Acta* **1989**, *72*, 123.

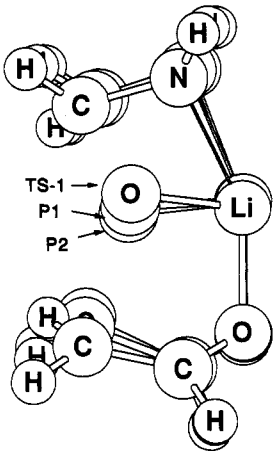

Bond Lengths	TS-1	P1	P2	17
C3-O1	1.547	1.706	1.781	2.906
C2-O1	2.181	1.749	1.533	1.387
Li-O1	1.896	1.914	1.942	1.744
Li-O2	1.750	1.855	1.901	1.944
C1-C2	1.368	1.449	1.483	1.513
C1-O2	1.296	1.240	1.230	1.228
C3-N	1.387	1.341	1.326	1.266
Displacements	0.0	2.2	3.4	---
Energies	-326.77283	-326.82861	-326.86345	-326.92787

Figure 8. TS-1 and two intermediate points (P1 and P2) along the reaction path toward products. IRC is at the HF/3-21G level; displacements and energies are given in atomic units and distances in angstroms.

the MP2 level of theory since geometry optimization with electron correlation correction affords a much better description of the O–N bond.[8d]

Although the transition-state geometry is clearly indicative of attack by the enolate carbon to afford the α-keto lithium alkoxide, the question that remains is whether the final product is preceded by an unstable epoxide intermediate **18** (found only at the HF/3-21G level) that undergoes rapid isomerization to the alkoxide (eq 2). This

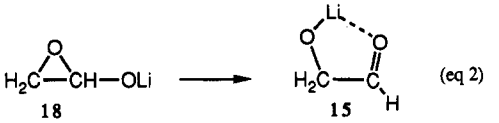

ambiguity can be removed by following the reaction path in internal coordinates[9f] from TS-1 down toward the product side. If it exists on the potential energy surface, a shallow energy minimum corresponding to the epoxide should be readily observable. However, the results indicate that TS-1 is connected to a structure resembling **17**, which is consistent with a direct S_N2 displacement on the oxaziridine to form the O_1–C_2 bond. Transition state TS-1 and two selected points P_1 and P_2, that are 35.0 and 56.9 kcal/mol "down hill" from the saddle point, are given in Figure 8. The TS is 97.3 kcal/mol above product complex **17**. These "snapshots" along the intrinsic reaction path clearly show shortening of the C–N bond as its π-character increases and the gradual decrease in the C_2–O_1 bond as the alkoxide bond in the product complex **17** is formed. The loss of π-character in the C–C bond and increase in the carbonyl π-bond (C_3–O_2) is also in evidence. Interestingly, both lithium–oxygen bond distances increase on the product side of the potential energy surface. However, the lithium transfer occurs late along the reaction coordinate. The O–C and O–N bonds in the oxaziridine have been elongated by 11 and 20%, respectively, in TS-1. A linear extrapolation of changes in bond distances suggests that the C–N π-bond is about 40% formed while the C–C π-bond character has only been reduced by about 20% at the transition state. Previous studies had suggested the

intermediacy of a hemiaminal resulting from addition of O_1 in **17** to the imino carbon (C_3). The IRC data suggest that such an equilibrium must take place after the transition state. Collapse of product complex **17** to epoxide **18** is also excluded since the latter compound does not exist at the 4-31+G level of theory but optimizes directly to α-keto lithium alkoxide **15**.

In summary, the transition state for oxygen transfer to the lithium enolate is quite similar to that for epoxidation of ethylene where the oxygen approached the alkene over one carbon atom.[8e] In consonance with existing descriptions of this type of reaction,[1,3] this oxygen atom transfer most likely involves a "closed" transition state with the metal cation providing a stabilizing binding interaction to both partially negatively charged oxygen atoms in the transition state. If coordination of the metal cation to one of the sulfonyl oxygen atoms is important, then TS-3 should be favored. The stereochemistry of the resulting α-hydroxy carbonyl compound is determined by a balance between this oxyanion stabilization and steric effects with no special stereoelectronic effects being apparent.

Acknowledgment. This work was supported in part by a grant from the National Institutes of Health (CA 47348-02) and Ford Motor Company. We are very thankful to the Pittsburgh Supercomputing Center, the Ford Motor Company, and the Computing Center at Wayne State University for generous amounts of computing time. One of us (J.L.A.) gratefully acknowledges a fellowship from the CIRIT of the Generalitat de Catalunya (Catalonia, Spain) which has made his stay at Wayne State University possible.

Registry No. **1** (X = Cl), 127184-05-8; **12**, 6827-26-5; **13**, 2053-29-4; **14**, 67285-39-6; **15**, 136586-89-5.

On the Reaction of (Vinylimino)phosphoranes and Related Compounds. 20.[1] Syntheses and Properties of Methanocyclodeca[*b*]pyridine Ring Systems

Nobuhiro Kanomata, Hiroyuki Kawaji, and Makoto Nitta*

Department of Chemistry, School of Science and Engineering, Waseda University, Shinjuku-ku, Tokyo 169, Japan

Received July 2, 1991

Novel 2-[(triphenyl- and 2-[(tributylphosphoranylidene)amino]-1,6-methano[10]annulenes (**8x,y**) and 3-[(triphenyl- and 3-[(tributylphosphoranylidene)amino]-1,6-methano[10]annulenes (**9x,y**) were generated by the Staudinger reaction of 2- and 3-azido-1,6-methano[10]annulenes (**5** and **6**). The compound **8x** was inert to α,β-unsaturated ketones, while compounds **8y** and **9y** were found to react with α,β-unsaturated ketones in enamine–alkylation process followed by aza–Wittig reaction and dehydrogenation to give 7,12- and 5,10-methanocyclodeca[*b*]pyridines **20a–f** and **26a,f**, respectively. The reactivity of **8** and **9** as well as the site selectivity of **9** was suggested by their ^{13}C NMR spectra, in which the carbon signals of the nucleophilic center appear at higher field as compared to those of 1,6-methano[10]annulene. Structural properties of **20a–f** and **26a,f** were examined by ^1H NMR and UV spectra. The ^1H NMR spectra analyzing aromatic characters clarified both remarkable reduction of a ring current and appearance of bond alternation as compared to the parent 1,6-methano[10]annulene (**1**). The UV spectra exhibiting a prolonged cyclic conjugation are in contrast to their 10π electron analogues, 1,6-methano[10]annulene (**1**) and quinoline derivatives.

The chemistry of bridged annulenes has been developed widely and deeply, ever since Vogel et al. reported the synthesis of 1,6-methano[10]annulene (**1**) as the first stable aromatic cyclodecapentaene.[2] The aromatic nature concerning diatropicity and bond alternation is largely influenced by the fusion of another aromatic ring. A typical example is 2,3-benzo-1,6-methano[10]annulene (**2**),[3] which shows both remarkable reduction of a ring current and bond alternation in the 10π electron unit as compared to **1**. The fusion of a heteroaromatic ring, on the other hand, is expected also to cause variations of the physical properties of **1**. Although various kinds of heterocyclic annulations are possible in principle, only a few examples have been reported.[4] Our interest focused on the synthesis and spectroscopic properties of methanocyclodeca[*b*]pyridines in relation to our previous studies of azaazulene vinylogues **3** and **4**.[5] Recently, our research group has been studying synthetic utilities of (vinylimino)phosphoranes, equivalents of primary enamine, for construction of various kinds of heterocycles.[6–9] A typical example is the reaction with α,β-unsaturated ketones resulting in the formation of pyridine derivatives[7] in enamine alkylation process followed by aza–Wittig reaction and dehydrogenation. In this paper, we describe the preparation and reactions of novel 2- and 3-(phosphoranylideneamino)-1,6-methano[10]-annulenes (**8x,y** and **9x,y**), and spectroscopic properties

(1) Part 19: Nitta, M.; Mori, S.; Iino, Y. *Tetrahedron Lett.*, in press.
(2) (a) Vogel, E.; Roth, H. D. *Angew. Chem.* **1964**, *76*, 145. (b) Vogel, E.; Klug, W.; Breuer, A. *Organic Syntheses*; Wiley: New York, 1988; Collect. Vol. VI, p 731. (c) Vogel, E. *Chem. Soc. Spec. Publ.* **1967**, No. 21, 113. (d) Vogel, E. *Proc. Robart A. Welch Found. Conf. Chem. Res.* **1968**, *12*, 215.
(3) Tanimoto, S.; Schäfer, R.; Ippen, J.; Vogel, E. *Angew. Chem., Int. Ed. Engl.* **1976**, *15*, 613.
(4) (a) Neidlein, R.; Lautenschläger, G. *Chem. Ber.* **1989**, *122*, 493. (b) Neidlein, R.; Tadesse, L. *Chem. Ber.* **1986**, *119*, 3862. (c) Neidlein, R.; Hartz, G. *Chem. Zeit.* **1984**, *108*, 366. (d) Brinker, U. H.; Jones, W. M. *Tetrahedron Lett.* **1976**, 577. Jones, M. W.; LaBar, R. A.; Brinker, U. H.; Gebert, P. H. *J. Am. Chem. Soc.* **1977**, *99*, 6379.
(5) Nitta, M.; Kanomata, N.; Masaru, T. *Tetrahedron Lett.* **1990**, *31*, 1291.
(6) Iino, Y.; Nitta, M. *J. Syn. Org. Chem. Jpn.* **1990**, *48*, 681.
(7) (a) Kobayashi, T.; Nitta, M. *Chem. Lett.* **1986**, 1549. (b) Kobayashi, T.; Iino, Y.; Nitta, M. *J. Chem. Soc. Jpn. (Nippon Kagaku Kaishi)* **1987**, 1237. (c) Iino, Y.; Nitta, M. *Bull. Chem. Soc. Jpn.* **1988**, *61*, 2235. (d) Kanomata, N.; Nitta, M. *Tetrahedron Lett.* **1988**, *29*, 5957; *J. Chem. Soc., Perkin Trans. 1* **1990**, 1119. (e) Nitta, M.; Soeda, H.; Iino, Y. *Bull. Chem. Soc. Jpn.* **1990**, *63*, 932. (f) Nitta, M.; Iino, Y. *J. Chem. Soc., Perkin Trans. 1* **1990**, 435. (g) Nitta, M.; Ohnuma, M.; Iino, Y. *Ibid.* **1991**, 1115.
(8) (a) Iino, Y.; Kobayashi, T.; Nitta, M. *Heterocycles* **1986**, *24*, 2437. (b) Iino, Y.; Hara, E.; Nitta, M. *Bull. Chem. Soc. Jpn.* **1989**, *62*, 1913.
(9) (a) Nitta, M.; Kobayashi, T. *Chem. Lett.* **1986**, 463. (b) Nitta, M.; Iino, Y.; Hara, E.; Kobayashi, T. *J. Chem. Soc., Perkin Trans. 1* **1989**, 51. (c) Nitta, M.; Iino, Y.; Kamata, K. *Heterocycles* **1989**, *29*, 1655.

0022-3263/92/1957-0618$03.00/0